

Prediction of Relaxed Woven Fabric Geometry Using Energy Method

Hadi Dabirian*, Ali Asghar Asgharian Jeddi, and Hadi Sharifi

Abstract- The aim of this study is to present a method to predict the geometrical parameters of relaxed fabrics using energy method. For this purpose, the potential energy of on-loom state of fabric is calculated and minimized to achieve theoretically the fully relaxed state. Tensile, bending and compression deformations of yarns are considered to obtain total strain energy of the unit-cell. Peirce's geometric model for woven fabrics is used in order to find geometrical equations. The predictions are compared with experimental data and the results are discussed.

Keywords: relaxed state, woven fabric, geometry, energy method

Nomenclature

p_0	Yarn spacing in loom state
p	Yarn spacing in relaxed state
L	Modular length of yarn in loom state
l	Modular length of yarn in relaxed state
d_0	Yarn diameter in loom state
d	Yarn diameter in relaxed state
δp	Change in yarn spacing
t	Linear density of yarn
E	Yarns modulus
θ	Weave angle in relaxed state
F	Acting force on the unit-cell of fabrics
δ	Change in yarn diameter due to compression
h	Crimp height of yarn
c	Crimp of yarn
B	Bending rigidity of yarn
κ	Yarn curvature
K	Bulk modulus of yarn
M	Bending moment
e	Strain of yarn

H. Dabirian, A.A. Asgharian Jeddi, and H. Sharifi
Department of Textile Engineering, Amirkabir University of Technology,
Tehran, Iran.

Correspondence should be addressed to H. Dabirian
e-mail: dabiryan@aut.ac.ir

I. INTRODUCTION

After removing fabrics from a loom, they are usually deformed due to residual stresses. Hence, it is essential that the fabrics to be relaxed before experimental measurements in order to determine the relationships which are independent of the detailed machine processing conditions [1]. The prediction of relaxed dimension of fabrics can be very useful in choosing the relaxation method and controlling relaxation conditions. The subject of fabric relaxation has been studied by many researchers [2-6]. Two states of relaxation, i.e. dry-relaxed and wet-relaxed, have been defined by Munden [2]. He suggested that the natural shape of the knitted loop was able to be determined by minimum energy conditions. Knapton *et al.* [3] investigated the dimensional properties of knitted wool fabrics and found that the fully-relaxed state was only achieved after the fabrics were thoroughly wetted-out, briefly hydro-extracted, and tumbled dried. Dimensional properties of fabrics have been studied by numerous researchers [4-7].

Over the years, energy method has been widely used to analyze the structure and mechanics of yarns, knitted fabrics, woven fabrics and nonwovens [8-16]. De Jong and Postle [12] proposed a general energy analysis of fabric mechanics which is independent of the fabric construction. Hearle *et al.* [13] reviewed the methods to investigate the mechanic of fabrics and suggested an energy-based approach to analyze the structure of fabrics. A theoretical model has been presented to predict the initial modulus of plain woven fabrics using Castigliano's theorem by Leaf and Kandil [14]. Dabirian *et al.* [15,16] studied the structure of warp-knitted fabrics using energy method. Sagar *et al.* [17] demonstrated the advantages of energy-based approach to solve fabric mechanics problems without the necessity of complex 3D finite element analysis. They presented a mechanical model to predict the tensile response of plain-woven fabric under in-plane uniaxial/biaxial loads. Different geometrical models have been presented for plain woven fabrics [18-21]. Manjunath and Behera [22] modeled the unit-cell of woven fabrics. They showed that the results computed from the models are close to the experimental values. Ferranto and Luo [23] modeled the plain woven fabrics from un-woven yarn configuration

using finite element method (FEM). Considering the geometry and material properties of yarns, they simulated the geometry of fabrics.

Although, the Peirce's geometrical model has unrealistic assumptions about the yarn's configuration in the structure of fabric, it is suitable to use in mechanical analysis because of simplicity. Therefore, it is used as the relaxed geometry of fabrics in this paper. In the present work, the minimization technique of energy is used to analyze the deformation of fabrics during the relaxation process.

A. Energy Approach

During fabric formation, constituent yarns are subjected to biaxial tension on the loom. The internal and external forces generate residual stresses needing to be eliminated in relaxation process. The fully relaxed state of fabrics can be defined as the minimum-energy shape of yarns within the fabric structure. It is well known that the total potential energy 'Π' of a conservative system is given by:

$$\pi = -W + U$$

Where U is the strain energy of the system and W is the potential of external forces.

Mathematically, the minimum of total energy is expressed as:

$$\frac{\partial \Pi}{\partial x_i} = 0 \quad i = 1, 2, \dots, n$$

Where, 'x₁, x₂, ..., x_n' are the generalized (independent) displacements associated with the generalized forces.

Fabrics in loom state are subjected to the biaxial tension due to the back-rest and temples position. The energies involved are associated with yarn extension, yarn bending and yarn compression. Therefore, the total energy stored in loom state of fabrics is:

$$U_T = U_E + U_B + U_C \tag{1}$$

Where;

U_E: Tensile strain energy,

U_B: Bending strain energy, and

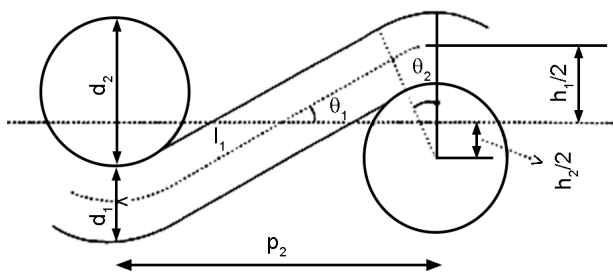


Fig. 1. Peirce's geometrical model for plain woven fabrics [17].

U_C: Compression strain energy.

It can be shown that [13]:

$$U_E = \frac{1}{2}(tEe^2)l \tag{2}$$

$$U_B = \frac{1}{2}(B\kappa^2)\delta l \tag{3}$$

$$U_C = \frac{1}{2}K\left(\frac{\delta d}{d}\right)^2 \tag{4}$$

In following, the subscripts 1 and 2 indicate the warp and weft yarns, respectively.

The external work under biaxial tension of fabric is given by:

$$W = F_1 \cdot \delta p_2 + F_2 \cdot \delta p_1 \tag{5}$$

The parameters such as yarn twisting and friction are neglected.

The fabric geometry treated here is Pierce's rigid model for plain woven fabrics which is shown in Fig. 1. The governing equations of this model are [17]:

$$p_1 = (l_2 - D\theta_2)\cos\theta_2 + D\sin\theta_2 \tag{6}$$

$$p_2 = (l_1 - D\theta_1)\cos\theta_1 + D\sin\theta_1 \tag{7}$$

$$h_1 = (l_1 - D\theta_1)\sin\theta_1 + D(1 - \cos\theta_1) \tag{8}$$

$$h_2 = (l_2 - D\theta_2)\sin\theta_2 + D(1 - \cos\theta_2) \tag{9}$$

$$h_1 + h_2 = d_1 + d_2 = D \tag{10}$$

It can be shown that [20]:

$$D = \left(d_{10}\sqrt{\frac{L_1}{l_1}} - \delta_1 \right) + \left(d_{20}\sqrt{\frac{L_2}{l_2}} - \delta_2 \right) \tag{11}$$

Considering these equations, the idea lgeometrical model has 10 unknown variables, i.e. p₁, p₂, l₁, l₂, h₁, h₂, θ₁, θ₂, d₁ and d₂, but there are five equations that connected them. Therefore, we need five more equations to find all of variables. The required equations can be obtained using principle of stationary potential energy. Since the variation of internal energies occurs during fabric relaxation, two states of fabrics are treated, loom state and relaxed state. The loom state of fabric is considered as initial state, and the relaxed state would be deformed state of fabrics. The geometrical variables of fabrics are categorized into two categories:

- Dependent variables which are related to the fabric structure, i.e. p₁, p₂, θ₁, θ₂, h₁ and h₂.

- Independent variables which are associated with constituent yarn, i.e. l_1, l_2, δ_1 and δ_2 .

Of all dependent variables, one of them should be considered as the independent parameter to solve the problems. Because of this, the weft distance (p_2) is treated as independent variable.

B. Calculation of Total Energy

It was aforementioned that the tensile, bending and compression of yarns within the fabric structure are considered. Using the strain energies equations and geometrical parameters of fabric, the tensile strain energy of fabrics under biaxial extension is given by:

$$U_E = \frac{1}{2}(E_1 t_1 L_1 e_1^2 + E_2 t_2 L_2 e_2^2) \quad (12)$$

Bending strain energy of fabric depends on the yarn curvature in the unit-cell. According to the shape of the cross-section, the curvature of yarns is changed. In circular cross-section, the length of the yarn is divided into free zone and contact zone. The free zone is a straight line, but the contact zone has an arc shape. It means that the yarn in contact zone is bent due the bending moment. The radii of yarn curvature can be assumed equal to $D/2$. Hence, the bending strain energy is expressed as bellow:

$$U_B = \frac{2}{D}(B_1 \theta_1 + B_2 \theta_2) \quad (13)$$

Yarns are flattened in the crossovers points due to the inter yarn pressure. Compression energy can be expressed in terms of transverse strain and compression modulus of yarns:

$$U_C = \frac{1}{2} \left(K_1 \left(\frac{\delta_1}{d_{01}} \right)^2 + K_2 \left(\frac{\delta_2}{d_{02}} \right)^2 \right) \quad (14)$$

And, the potential of external loads is obtained as follow:

$$W = -F_1(p_2 - p_{02}) - F_2(p_1 - p_{01}) \quad (15)$$

Consequently, the total potential energy of the unit-cell under biaxial tension is:

$$\begin{aligned} \Pi = & \frac{1}{2}(E_1 t_1 L_1 e_1^2 + E_2 t_2 L_2 e_2^2) + \frac{2}{D}(B_1 \theta_1 + B_2 \theta_2) + \\ & \frac{1}{2} \left(K_1 \left(\frac{\delta_1}{d_{01}} \right)^2 + K_2 \left(\frac{\delta_2}{d_{02}} \right)^2 \right) - F_1(p_2 - p_{02}) + F_2(p_1 - p_{01}) \end{aligned} \quad (16)$$

It is possible to obtain force-equilibrium equations using the principle of stationary potential energy. Minimizing the total energy with respect to five independent variables i.e.

p_2, l_1, l_2, δ_1 and δ_2 gives the five required equations to obtain the unknown parameters (see Appendix I).

$$\begin{aligned} \left(\frac{\partial \Pi}{\partial p_2} \right)_{l_1, l_2, \delta_1, \delta_2} &= 0 \\ F_1 + F_2 \left(\frac{\tan \theta_2}{\tan \theta_1} \right) &= \left(\frac{2B_1}{D} \right) \left(\frac{1}{\sin \theta_1 (D\theta_1 - l_1)} \right) + \left(\frac{2B_2}{D} \right) \left(\frac{1}{\tan \theta_1 \cos \theta_2 (D\theta_1 - l_1)} \right) \\ \left(\frac{\partial \Pi}{\partial l_1} \right)_{p_1, l_2, \delta_1, \delta_2} &= 0 \end{aligned} \quad (17)$$

$$\begin{aligned} F_2 \left[\frac{\tan \theta_2 \cos \theta_1}{\tan \theta_1} \right] &= \left(\frac{E_1 t_1 (l_1 - L_1)}{L_1} \right) + \left(\frac{2B_1}{D} \right) \\ \left(\frac{\cos^2 \theta_1}{p_2 \sin \theta_1 - D \sin^2 \theta_1} \right) &+ \left(\frac{2B_2}{D} \right) \left(\frac{\cos^3 \theta_1 (D\theta_1 - l_1)}{\cos \theta_2 (D\theta_2 - l_2) (p_2 \sin \theta_1 - D \sin^2 \theta_1)} \right) \\ &+ \left(\frac{(2B_1 \theta_1 + 2B_2 \theta_2)}{D^2} \right) + \left(\frac{d_{01}}{2\sqrt{l_1^3}} \right) \end{aligned} \quad (18)$$

$$\begin{aligned} \left(\frac{\partial \Pi}{\partial l_2} \right)_{p_2, l_1, \delta_1, \delta_2} &= 0 \\ F_2 \cos \theta_2 &= (E_2 t_2 (l_2 - L_2) / L_2) + \left(\frac{2B_1}{D} \right) \left(\frac{\cos^3 \theta_2 (D\theta_2 - l_2)}{\cos \theta_1 (D\theta_1 - l_1) (p_1 \sin \theta_2 - D \sin^2 \theta_2)} \right) \\ &+ \left(\frac{2B_2}{D} \right) \left(\frac{\cos^2 \theta_2}{p_1 \sin \theta_2 - D \sin^2 \theta_2} \right) + \left(\frac{(2B_1 \theta_1 + 2B_2 \theta_2)}{D^2} \right) \left(\frac{d_{02}}{2\sqrt{l_2^3}} \right) \end{aligned} \quad (19)$$

$$\begin{aligned} \left(\frac{\partial \Pi}{\partial \delta_1} \right)_{x_1, l_1, l_2, \delta_2} &= 0 \\ -F_2 \left(\frac{\tan \theta_2 \cos^2 \theta_1}{\sin \theta_1} \right) &= \left(\frac{K_1 \delta_1}{d_{01}^2} \right) - \left(\frac{2B_1}{D} \right) \left(\frac{2 \cos \theta_1 \sqrt{l_1^3}}{d_{01} \sin \theta_1 (D\theta_1 - l_1)} \right) \\ &- \left(\frac{2B_2}{D} \right) \left(\frac{2\sqrt{l_1^3}}{d_{01}} \right) \left(\frac{\cos^2 \theta_1}{\cos \theta_2 \sin \theta_1 (D\theta_2 - l_2)} \right) + \left(\frac{(2B_1 \theta_1 + 2B_2 \theta_2)}{D^2} \right) \end{aligned} \quad (20)$$

$$\begin{aligned} \left(\frac{\partial \Pi}{\partial \delta_2} \right)_{x_1, l_1, l_2, \delta_2} &= 0 \\ -F_2 \left(\frac{2\sqrt{l_1^3} \cos \theta_2 \sin \theta_2}{d_{02} \sin \theta_1} \right) &= \left(\frac{K_2 \delta_2}{d_{02}^2} \right) - \left(\frac{2B_1}{D} \right) \left(\frac{2\sqrt{l_2^3}}{d_{02}} \right) \left(\frac{\cos^2 \theta_2}{\cos \theta_1 \sin \theta_2 (D\theta_1 - l_1)} \right) \\ &- \left(\frac{2B_2}{D} \right) \left(\frac{2\sqrt{l_1^3} \cos \theta_2}{d_{02} \sin \theta_1 (D\theta_2 - l_2)} \right) + \left(\frac{(2B_1 \theta_1 + 2B_2 \theta_2)}{D^2} \right) \end{aligned} \quad (21)$$

C. Calculation of Geometrical Parameters of Fabric

It was aforementioned that the loom state of fabrics is the initial state of system. Therefore, the geometrical parameters of fabrics in this state (i.e. $p_{01}, p_{02}, l_{01}, l_{02}, h_{01}, h_{02}, \theta_{01}, \theta_{02}$) and yarns characteristics (i.e. $d_{01}, d_{02}, E_1, E_2, B_1$ and B_2) are the known parameters. The geometrical parameters of relaxed state (i.e. $p_1, p_2, l_1, l_2, d_1, d_2, h_1, h_2, \theta_1, \theta_2$) are the unknown parameters which should be calculated as the results of

TABLE I
DETAILS OF THE WEFT YARNS

Fabric group	Material	Linear density
		(Tex)
Y1P	Cotton	34.5
Y2P	Polyester	27.5

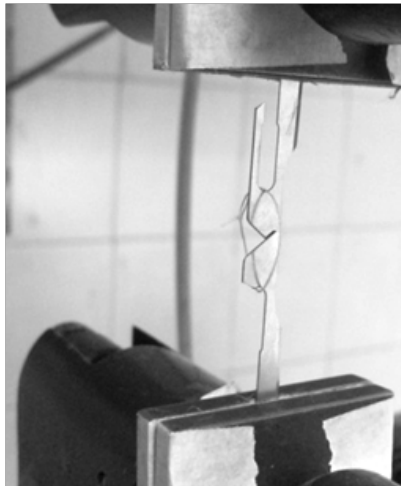


Fig. 2. Measuring the flexural rigidity using ring loop method.

minimizing the potential energy of system. By solving simultaneous Eqs. (6)–(10) and (17)–(21) for the geometric derivative terms, the unknown variables are obtained. Since, these equations are non-linear the Newton-Raphson method can be used to solve them (see Appendix II).

II. EXPERIMENTAL

A. Materials and Methods

To verify the proposed method, six types of plain woven fabrics were produced using different yarns on a SMIT Rapier TP400 weaving loom. The warp (50.4-tex cotton) was common to all groups, but the weft was varied according to the scheme shown in Table I.

Within each group, three fabrics with different numbers

TABLE II
RESULTS OF YARN'S FLEXURAL RIGIDITY

Yarn type	d/L*	Average load	Flexural rigidity
		(N)	(mN.mm ²)
Weft-type Y1	0.074	0.021	2.18
Weft-type Y2	0.074	0.026	3.09
Warp	0.074	0.034	3.67

*d: loop diameter; L: length of deformed loop

of picks/cm were woven. The geometrical parameters of fabrics on loom were measured. As shown in Fig. 2, the yarn flexural rigidity was measured using ring loop method developed by Owen and Riding [24]. The results of flexural rigidity of yarns are presented in Table II.

The warp and weft thread-spacing in the fabrics were measured by counting the number of warps and wefts in a 10 cm length of cloth. Using measured values and geometrical equation the modular lengths of the yarns was obtained. The tensile modulus of yarns was measured using an Instron tensile tester based on ASTM D2256. The forces in the warp and weft directions (F_1 and F_2) were measured using a tensionmeter on the loom. For measuring F_1 , the tensionmeter was set on the warp yarns between backrest and head. But, in order to measure F_2 , a simulated state was designed on the Instron tensile tester in which the fabrics were stretched up to the initial dimension and the load was recorded. These data are summarized as the characteristic of initial state of fabric in Table III.

Putting the values of the Table III into the derived equations, the geometrical parameters of relaxed fabrics (deformed state) are calculated. To solve the equations, the Newton-Raphson method was used on the MATLAB v R2007. The theoretical results of the model have been shown in Table IV. To get the relaxed state empirically, the fabrics were removed from the loom and laid on a flat surface for 24 h. After that, the samples were washed at 90 °C for 1 h. The

TABLE III
CHARACTERISTICS OF THE INITIAL STATE (ON LOOM)

Fabric code	t_1 (text)	t_2 (tex)	E_1 (N/tex)	E_2 (N/tex)	B_1 (mN.mm ²)	B_2 (mN.mm ²)	P_{01} (mm)	P_{02} (mm)	F_1 (N)	F_2 (N)
Y1P1	34.4	50.4	3836	4498	3.67	2.18	0.625	1.00	0.78	0.14
Y1P2	34.4	50.4	3836	4498	3.67	2.18	0.625	0.71	0.82	0.09
Y1P3	34.4	50.4	3836	4498	3.67	2.18	0.625	0.55	0.83	0.08
Y2P1	27.5	50.4	3836	1668	3.67	3.09	0.625	1.00	0.78	0.16
Y2P2	27.5	50.4	3836	1668	3.67	3.09	0.625	0.71	0.85	0.1
Y2P3	27.5	50.4	3836	1668	3.67	3.09	0.625	0.55	0.85	0.1

TABLE IV
THE ORETICAL RESULTS OF THE DEFORMED STRUCTURE (RELAXED STATE)

Fabric code	p_1 (mm)	p_2 (mm)	l_1 (mm)	l_2 (mm)	θ_1 (rad)	θ_2 (rad)	h_1 (mm)	h_2 (mm)
Y1P1	0.566	0.858	0.935	0.565	0.450	0.003	0.371	0.003
Y1P2	0.573	0.578	0.700	0.573	0.695	0.009	0.369	0.005
Y1P3	0.577	0.421	0.553	0.58	0.936	0.106	0.059	0.443
Y2P1	0.573	0.875	0.946	0.573	0.414	0.007	0.351	0.004
Y2P2	0.577	0.576	0.681	0.578	0.639	0.024	0.342	0.013
Y2P3	0.584	0.458	0.573	0.585	0.791	0.075	0.313	0.042

geometrical parameters of fabrics were measured after 24 h. For measuring the modular lengths, fabric samples with dimension of 10×10 cm² were prepared, and a number of weft and warp yarns were removed from their structure. In order to decrimp yarns, a load of 10 g was applied on yarns and the length of yarns was recorded as modular lengths. Considering the distance between lengths of yarn and dimension of fabrics, the crimp percentage of the yarns and modular lengths were calculated. Similar to what was done for the initial state, the geometrical parameters of relaxed state were obtained.

III. RESULTS AND DISCUSSION

In order to check the accuracy of the model, the predicted geometrical parameters of fabrics were compared with the experimental results. For this purpose, the predicted values including thread spacing (P), modular length (l), crimp height (h), and weave angle (θ) were compared with the experimental data. To compare the prediction of the model with the experimental results, the geometrical parameters of fabrics in both weft and warp directions are considered and discussed.

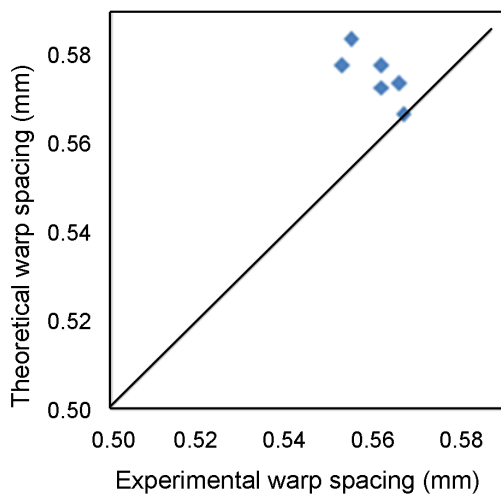


Fig. 3. Relationship between the theoretical and experimental warp spacing data.

TABLE V
WARP SPACING VALUES

Fabric code	Theoretical data (mm)	Experimental data (mm)	Error (%)
Y1P1	0.566	0.567	0.2
Y1P2	0.573	0.562	-2.0
Y1P3	0.578	0.553	-4.5
Y2P1	0.574	0.566	-1.4
Y2P2	0.578	0.562	-2.8
Y2P3	0.584	0.555	-5.2

A. Warp Spacing (P_1)

Table V provides comparison between the theoretical and experimental warp spacing values for different fabrics. Considering the values of this table, it can be seen that the error percentage increases by increasing the weft density of samples. Increment of weft density may lead to the deformation of yarn cross-section, which has been ignored in this research. In general, there is a reasonable agreement between the theoretical and experimental results.

The points plotted in Fig. 3 show that the predicted warp spacing is generally more than its experimental value. This may be due to the error calculation of the model which is associated with the calculation method.

B. Weft Spacing (P_2)

The theoretical and experimental values of weft spacing shown in Table VI demonstrate that the predicted values are approximately close to the experiments. In most of the

TABLE VI
PICK SPACING VALUES

Fabric code	Theoretical data (mm)	Experimental data (mm)	Error (%)
Y1P1	0.854	0.812	5.2
Y1P2	0.578	0.573	0.8
Y1P3	0.422	0.477	11.6
Y2P1	0.875	0.814	7.5
Y2P2	0.577	0.596	3.2
Y2P3	0.458	0.487	5.8

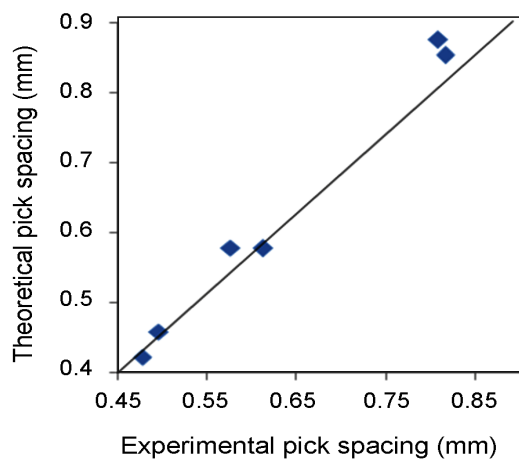


Fig. 4. Relationship between the theoretical and experimental pick spacing values.

fabrics, except for Y1P3, the error percentages are less than 10%.

As can be seen in Fig. 4, the distribution of points around the 45°-line is uniform.

C. Modular Length of Warp (l_1)

According to Table VII, the predicted modular lengths of warps are very close to the experimental results. Among the geometrical parameters, the modular length has the least variation during the relaxation process. It means that the energy differentiation in terms of modular length variation would be small.

As can be seen from the points plotted in Fig. 5, there is a quite good agreement between the theory and experiment of modular length of warps.

D. Modular Length of Weft (l_2)

The values of Table VIII confirm that the model is able to predict the geometrical parameters of fabrics in relaxation state. Contrary to parameters obtained previously, the experimental values of modular length for all samples are more than the theoretical values of modular length. The correlation between the theoretical and experimental

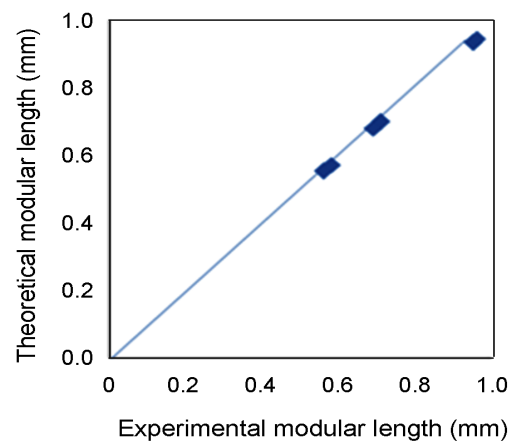


Fig. 5. Relationship between the theoretical and experimental modular length of warp.

modular length of weft yarns has been shown in Fig. 6.

E. Weave Angle in Warp Direction (q_1)

The predicted values of weave angle in warp direction are far from its experimental data (Table IX). This can be attributed to the relaxation process of fabrics. During the relaxation process, the swelling of fiber and yarn produced on wetting cause to increase the yarn diameter which has not been taken into account in this work. In the other hand, the weave angle considerably depends on the geometrical assumptions. Since the weave angle is significantly affected by the values of other parameters, unreal assumption regarding to the fabrics structure can deviate the values from the real case. The assumptions including circular cross-section, uniform structure along the longitudinal direction, perfect flexibility, and incompressibility are all unrealistic, leading to increase the error level. These facts lead to change the weave angle. Fig. 7 shows the correlation between the experimental and theoretical results.

F. Weave Angle in Weft Direction (q_2)

Referring to the values of Table X, the results obtained from the model are very far from the experimental

TABLE VII
MODULAR LENGTH OF WARP (L_1)

Fabric code	Theoretical data (mm)	Experimental data (mm)	Error (%)
Y1P1	0.935	0.954	1.99
Y1P2	0.700	0.713	1.82
Y1P3	0.553	0.563	1.78
Y2P1	0.946	0.963	1.77
Y2P2	0.681	0.693	1.73
Y2P3	0.573	0.583	1.72

TABLE VIII
MODULAR LENGTH OF WEFT (L_2)

Fabric code	Theoretical data (mm)	Experimental data (mm)	Error (%)
Y1P1	0.565	0.577	-2.12
Y1P2	0.573	0.583	-1.75
Y1P3	0.580	0.594	-2.41
Y2P1	0.573	0.583	-1.75
Y2P2	0.578	0.588	-1.73
Y2P3	0.585	0.594	-1.54

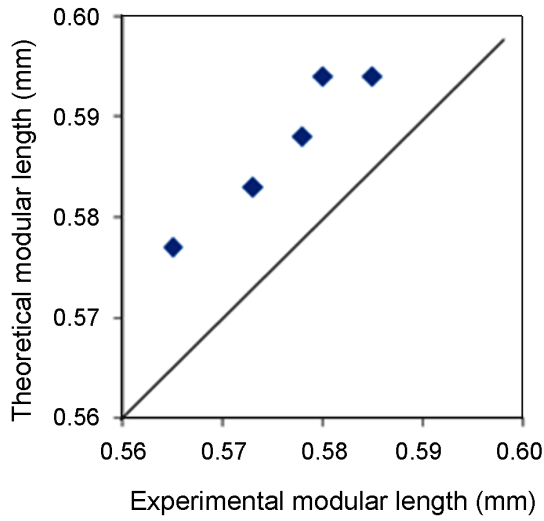


Fig. 6. Relationship between the theoretical and experimental modular length of weft.

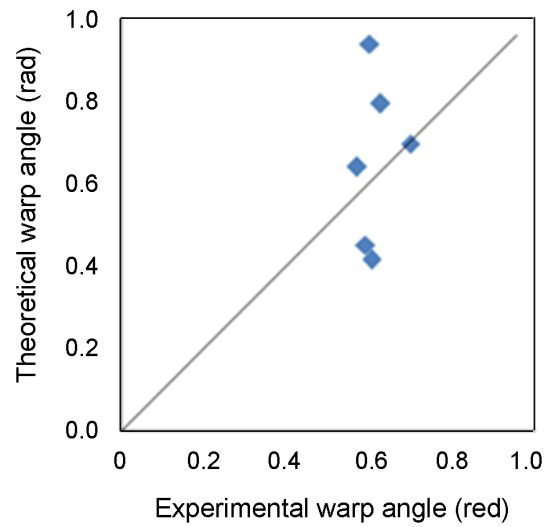


Fig. 7. Relationship between the theoretical and experimental weave angle values in warp direction.

results of weave angle in weft direction. The reason of these differences is the same as those mentioned for the weave angle in warp direction. As was pointed out earlier, the swelling in relaxation process affects considerably the prediction results of model obtained for weave angle (Fig. 8). As shown in Fig. 9, the theoretical data of weave angle in weft direction are considerably smaller than the weave angle experimental values.

G. Weft Crimp Height (h_w)

It can be inferred from the data presented in Table XI that the theoretical values of weft crimp height (except for Y1P3) are considerably smaller than those found experimentally. The relationship between the theoretical and experimental results is plotted as points in Fig. 10. There is only a slight variation in weft crimp height during the relaxation process since the weft-wise shrinkage of fabrics is not significant.

H. Warp Crimp Height (h_p)

Considering the experimental and theoretical values of warp crimp height issued in Table XII, we can say, the

TABLE IX
WAVE ANGLE IN WARP DIRECTION (θ_w)

Fabric code	Theoretical data (rad)	Experimental data (rad)	Error (%)
Y1P1	0.450	0.5914	23.9
Y1P2	0.695	0.6990	0.6
Y1P3	0.936	0.6005	-55.9
Y2P1	0.414	0.6051	31.6
Y2P2	0.639	0.5705	-12.0
Y2P3	0.791	0.6279	-26.0

TABLE X
WEAVE ANGLE IN WEFT DIRECTION (θ_2)

Fabric code	Theoretical data (rad)	Experimental data (rad)	Error (%)
Y1P1	0.003	0.1878	-
Y1P2	0.009	0.2734	-
Y1P3	0.106	0.3851	-
Y2P1	0.007	0.2451	-
Y2P2	0.024	0.3042	-
Y2P3	0.075	0.3749	-

model gives a reasonable approximation of this parameter, except Y1P3. It is well known that the fabrics have considerable warp-wise shrinkage which leads to the large variation of warp crimp height. This is probably the

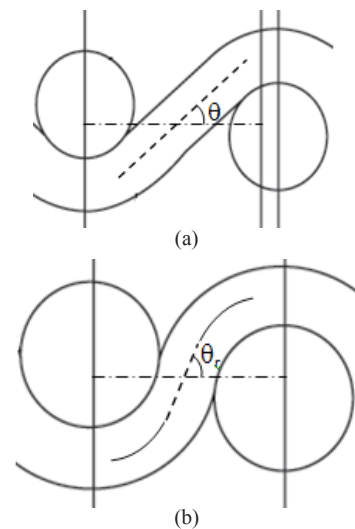


Fig. 8. Yarn diameter variation on wetting: (a) before swelling and (b) after swelling.

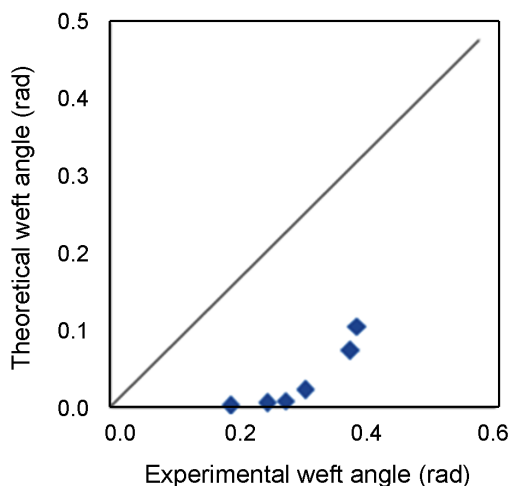


Fig. 9. Relationship between the theoretical and experimental weave angle values in weft direction.

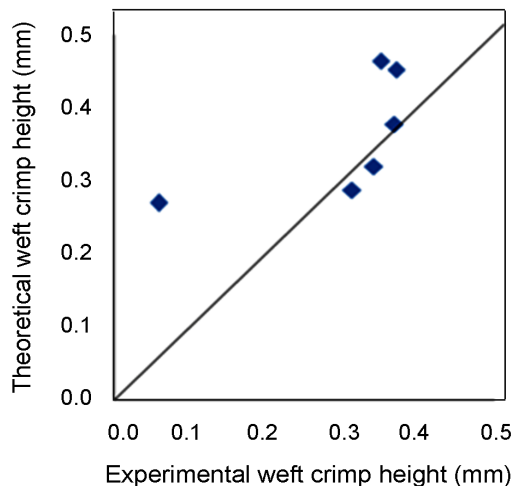


Fig. 11. Relationship between the theoretical and experimental warp crimp height values.

TABLE XI
WEFT CRIMP HEIGHT (H_2)

Fabric code	Theoretical data (mm)	Experimental data (mm)	Error (%)
Y1P1	0.003	0.1004	-
Y1P2	0.005	0.1448	-
Y1P3	0.443	0.2008	-
Y2P1	0.004	0.1308	-
Y2P2	0.013	0.1612	-
Y2P3	0.042	0.1962	-

TABLE XII
WARP CRIMP HEIGHT (H_1)

Fabric code	Theoretical data (mm)	Experimental data (mm)	Error (%)
Y1P1	0.371	0.4528	-22.0
Y1P2	0.369	0.3776	-2.3
Y1P3	0.059	0.2701	-357.8
Y2P1	0.351	0.4643	-32.3
Y2P2	0.342	0.3206	6.3
Y2P3	0.313	0.2883	7.9

reason of obtaining theoretical results of warp crimp height closer to the experiments than that of weft crimp height. The relationship between the theoretical and experimental warp crimp height values has been shown in Fig. 11.

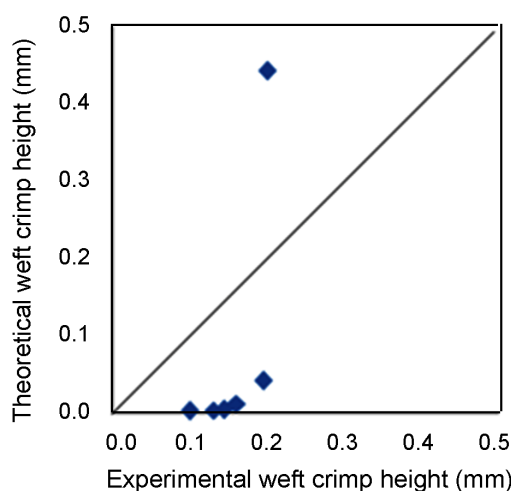


Fig. 10. Relationship between the theoretical and experimental pick spacing values.

IV. CONCLUSION

A mechanical model was generated to predict the geometrical parameters of relaxed state of woven fabrics using energy method. Assuming that the relaxed state of fabric is mathematically equivalent to the condition of minimum energy, the total potential energy of fabrics on loom was calculated and minimized. Comparison of theoretical and experimental results showed that the model could adequately predict warp and weft spacing in relaxed state, so that the maximum errors of prediction were about 5 and 11 percent, respectively. Also, the difference between the theoretical and experimental values of modular length of yarns in the unit-cell (l_1 and l_2) showed that the maximum errors were about 1.9 and 2.4 percent. The precision of modular length prediction could be attributed to the accuracy of experimental measurement. While, the predicted values of weave angle and crimp height were far from the experimental results due to difficulties and assumptions made in measuring these parameters. In some cases the error of prediction was about 50 percent. It is well known that the yarn spacing and modular length of yarns are more important commercially parameters compared to

weave angle and crimp height of yarns. It is concluded that the model can be applicable to predict the relaxed parameter of fabrics, practically. It is possible to improve the results of the model by taking into account the deformation of yarns cross-section in fabric structure.

ACKNOWLEDGEMENT

This work was supported by the Amirkabir University of Technology.

REFERENCES

- [1] R. Postle, G.A. Carnaby, and S. DeJong, *The Mechanics of Wool Structures*, New York: John Wiley & Sons, 1988, pp. 207-209.
- [2] D.L. Munden, "The geometry and dimensional properties of plain-knitted fabrics", *J. Text. Inst.*, vol. 50, T448, 1959.
- [3] J.J.F. Knapton, F.J. Ahrens, W.W. Ingenthron, and W. Fong, "The dimensional properties of knitted wool fabrics: part I: the plain-knitted structure", *Text. Res. J.*, vol. 38, pp. 999-1012, 1968.
- [4] R. Postle, "Dimensional stability of plain-knitted fabrics", *J. Text. Inst.*, vol. 59, no. 2, pp. 65-77, 1968.
- [5] J.A. Smirfitt, "Worsted 1×1 rib fabrics, part I: dimensional properties", *J. Text. Inst.*, vol. 56, no. 5, pp. T248-T259, 1965.
- [6] A.A.A. Jeddi and F. Zareian, "Ideal model for 1 × 1 rib fabric taking into account yarn swelling: guidelines for the use of ultrasonic relaxation", *J. Text. Inst.*, vol. 97, no. 6, pp. 475-482, 2006.
- [7] S. Mukherjee, S.C. Ray, and S.K. Punj, "A study on dimensional parameters of 1×1 rib produced on a flat bed double jersey knitting machine using ultrasonic technique", *Indian J. Fiber Text. Res.*, vol. 37, pp. 60-67, 2012.
- [8] L.R.G. Treloar and G. Riding, "A theory of the stress-strain properties of continuous-filament yarns", *J. Text. Inst.*, vol. 54, pp. T156-T170, 1963.
- [9] P. Grosberg and S. Kedia, "The mechanical properties of woven fabrics-part I: the initial load extension modulus of woven fabric", *Text. Res. J.*, vol. 36, pp. 70-79, 1966.
- [10] J.W.S. Hearle and A. Newton, "Nonwoven fabric studies: part XIV: derivation of generalized mechanics by the energy method", *Text. Res. J.*, vol. 37, pp. 778-797, 1967.
- [11] S. De Jong and R. Postle, "An energy analysis of the mechanics of weft-knitted fabrics by means of optimal-control theory part I: the nature of loop-interlocking in the plain knitted structure", *J. Text. Inst.*, vol. 68, no. 10, pp. 307-315, 1977.
- [12] S. De Jong and R. Postle, "A general energy analysis of fabric mechanics using optimal control theory", *Text. Res. J.*, vol. 48, pp. 127-35, 1978.
- [13] J.W.S. Hearle, P. Potluri, and V.S. Thammandra, "Modeling fabric mechanics", *J. Text. Inst.*, vol. 92, no. 3, pp. 53-69, 2001.
- [14] G.A.V. Leaf and K.H. Kandil, "The initial load-extension behavior of plain-woven fabrics", *J. Text. Inst.*, vol. 71, no. 1, pp. 1-7, 1980.
- [15] H. Dabiryan, A.A.A. Jeddi, and A. Rastgoo, "Analysis of warp knitted fabric structure, part II: theoretical study on initial modulus of warp knitted fabrics (tricot, locknit and satin)", *J. Text. Inst.*, vol. 103, no. 9, pp. 997-1011, 2012.
- [16] H. Dabiryan, A.A.A. Jeddi, and A. Rastgoo, "Analysis of warp knitted fabric structure, part III: theoretical study on initial modulus of warp knitted fabrics (reverse locknit, three- and four-needle sharkskin)", *J. Text. Inst.*, vol. 103, no. 11, pp. 1213-1227, 2012.
- [17] T.V. Sagar, P. Potluri, and J.W.S. Hearle, "Meso-scale modeling of interlaced fiber assemblies using energy method", *Computational Mater. Sci.*, vol. 28, pp. 49-62, 2003.
- [18] F.T. Peirce, "The geometry of cloth structure", *J. Text. Inst.*, vol. 28, no. 3, pp. T45-T96, 1937.
- [19] A. Kemp, "An extension of peirce's cloth geometry to the treatment of nonlinear thread", *J. Text. Inst.*, vol. 49, no. 1, pp. T44-T48, 1958.
- [20] J.W.S. Hearle and W.J. Shanahan, "An energy method for calculations in fabric mechanics; part II: examples of the application of the method to woven fabrics", *J. Text. Inst.*, vol. 69, no. 4, pp. 92-100, 1978b.
- [21] M.J. Avanaki, A.A.A. Jeddi, and A. Rastgoo, "A novel approach in geometrical-mechanical analysis of plain woven fabrics; initial load-extension behavior", *J. Text. Polym.*, vol. 2, no. 1, pp. 34-44, 2014.
- [22] R.N. Manjunath and B.K. Behera, "Modelling the geometry of the unit cell of woven fabrics with integrated stiffener sections", *J. Text. Inst.*, vol. 108, no. 11, pp. 2006-2012, 2017.
- [23] J.S. Ferranto and S.Y. Luo, "Finite element modeling of plain weave fabric from an un-woven initial yarn configuration", *Strength Mater.*, vol. 47, no. 6, pp. 903-911, 2015.
- [24] J.D. Owen and G. Riding, "The weighted-ring stiffness test", *J. Text. Inst.*, vol. 55, no. 8, pp. T414-T417, 1964.